

Non-Born-Oppenheimer Liouville-von Neumann Dynamics. Evolution of a Subsystem Controlled by Linear and Population-Driven Decay of Mixing with Decoherent and Coherent Switching

Chaoyuan Zhu, Ahren W. Jasper, and Donald G. Truhlar*

*Department of Chemistry and Supercomputing Institute, 207 Pleasant Street S.E.,
University of Minnesota, Minneapolis, Minnesota 55455-0431*

Received February 3, 2005

Abstract: Electronic energy flow in an isolated molecular system involves coupling between the electronic and nuclear subsystems, and the coupled system evolves to a statistical mixture of pure states. In semiclassical theories, nuclear motion is treated using classical mechanics, and electronic motion is treated as an open quantal system coupled to a “bath” of nuclear coordinates. We have previously shown how this can be simulated by a time-dependent Schrödinger equation with coherent switching and decay of mixing, where the decay of mixing terms model the dissipative effect of the environment on the electronic subdynamics (i.e., on the reduced dynamics of the electronic subsystem). In the present paper we reformulate the problem as a Liouville-von Neumann equation of motion (i.e., we propagate the reduced density matrix of the electronic subsystem), and we introduce the assumption of first-order linear decay. We specifically examine the cases of equal relaxation times for both longitudinal (i.e., population) decay and transverse decay (i.e., dephasing) and of longitudinal relaxation only, yielding the linear decay of mixing (LDM) and the population-driven decay of mixing (PDDM) schemes, respectively. Because we do not generally know the basis in which coherence decays, that is, the pointer basis, we judge the semiclassical methods in part by their ability to give good results in both the adiabatic and diabatic bases. The accuracy in the prediction of physical observables is shown to be robust not only with respect to basis but also with respect to the way in which demixing is incorporated into the master equation for the density matrix. The success of the PDDM scheme is particularly interesting because it incorporates the least amount of decoherence (i.e., the PDDM scheme is the most similar of the methods discussed to the fully coherent semiclassical Ehrenfest method). For both the new and previous decay of mixing schemes, four kinds of decoherent state switching algorithms are analyzed and compared to one another: natural switching (NS), self-consistent switching (SCS), coherent switching (CS), and globally coherent switching (GCS). The CS formulations are examples of a non-Markovian method, in which the system retains some memory of its history, whereas the GCS, SCS, and NS schemes are Markovian (time local). These methods are tested against accurate quantum mechanical results using 17 multidimensional atom–diatom test cases. The test cases include avoided crossings, conical interactions, and systems with noncrossing diabatic potential energy surfaces. The CS switching algorithm, in which the state populations are controlled by a coherent stochastic algorithm for each complete passage through a strong interaction region, but successive strong-interaction regions are not mutually coherent, is shown to be the most accurate of the switching algorithms tested for the LDM and PDDM methods as well as for the previous decay of mixing methods, which are reformulated here as Liouville-von Neumann equations with nonlinear decay of mixing (NLDM). We also demonstrate that one variant of the PDDM method with CS performs almost equally well in the adiabatic and diabatic representations, which is a difficult objective for semiclassical methods. Thus decay of mixing methods provides powerful mixed quantum-classical methods for modeling non-Born-Oppenheimer polyatomic dynamics including photochemistry, charge-transfer, and other electronically nonadiabatic processes.

I. Introduction

The Born-Oppenheimer approximation assumes that the relatively slow motion of nuclei can be separated from the

faster electronic motion, and thus the nuclei effectively move on a single electronically adiabatic potential energy surface. Due to the prohibitive computational expense of using quantum mechanics to treat the nuclear motion of large systems (say, for systems larger than four atoms), molecular

* Corresponding author e-mail: truhlar@umn.edu.

dynamics (MD) simulations often treat the nuclear motion using classical mechanics. The combination of quantal electronic motion and classical nuclear motion for such a Born-Oppenheimer process leads to the classical trajectory¹ or quasiclassical trajectory² (QCT) method when applied to gas-phase systems or the molecular dynamics (MD) method³ when applied to condensed-phase systems. However, when the system has low-lying excited electronic states, the Born-Oppenheimer approximation may break down, and non-adiabatic transitions may couple nuclear motion in the various low-lying electronic states. To extend the QCT and MD methods to treat nonadiabatic transitions caused by breakdown of the Born-Oppenheimer approximation, two new issues arise, namely that nuclear motion is governed by two or more potential energy surfaces and that these surfaces are coupled, leading to non-Born-Oppenheimer trajectories. Various mixed quantum-classical methods have been proposed to incorporate electronically nonadiabatic dynamics,⁴ and in this article we call these semiclassical methods because some degrees of freedom (the electronic ones) are quantal, and others (the nuclear ones) are classical.

A general problem faced by all mixed quantum-classical approaches is the problem of how to couple classical nuclear motion to quantal electronic motion to best simulate the true overall dynamics, which is of course fully quantal. If the goal is to calculate detailed quantum state-to-state transitions, then one must include all phase and interference effects, which is difficult in an approximate calculation; however, most experimentally interesting observables in practical problems involving photochemistry are highly averaged quantities in which much of the phase and interference information is washed out. In most applications the goal is to develop general methods to calculate these averaged quantities, such as total quenching cross sections or rate constants for photoinduced reactions. For this reason it is sufficient to consider predicting the diagonal elements of the density matrix⁵ because they control the final state populations. There is, however, a second reason to formulate the problem in terms of the density matrix, namely that the electronic degrees of freedom constitute a subsystem, and the Liouville-von Neumann equation of motion^{6–16} (also called the quantum Liouville equation) provides a theoretical framework for propagating the density matrix of a subsystem. In particular it provides a widely accepted language for characterizing relaxation and decoherence (also described as dissipation and dephasing). Relaxation and decoherence of the electronic degrees of freedom in a “bath” of nuclear degrees of freedom can be and have been described in wave function language,^{15,17,18} but in the present article, following earlier work,^{8–16} we use density matrix language.

In formulating the semiclassical aspect of the problem, we limit our attention to methods that involve independent trajectories since coupling trajectories together, although it may better simulate a wave packet,¹⁹ raises unsolved questions of computational efficiency and how best to treat the coupling. Independent-trajectory methods may be classified into two main categories: (1) trajectory surface hopping (TSH) methods^{20–33} in which the classical motion at any given time is governed by one or another potential energy

surface (each associated with a given electronic state in a given representation), and this motion is interrupted by hops (jumps, switches) between surfaces and/or bifurcations into two or more independent daughter trajectories (on different surfaces), each of which can further hop or bifurcate; and (2) self-consistent potential (SCP) methods^{15–18,34–48} in which trajectories are governed by a weighted averaged of the coupled potential energy surfaces, where the weight changes continuously as a function of time. The most consistent of the TSH methods are based on Tully’s fewest-switches (TFS) criterion,²⁴ which attempts to make the electronic probability distribution averaged over an ensemble of trajectories equal to the probability distribution computed from the electronic density matrix. The most straightforward of the SCP methods is the semiclassical Ehrenfest (SE) method.⁴⁰

Some TSH methods are reasonably accurate for treating classical allowed transitions, where energy conservation is achieved during hops or in daughter trajectories by adjusting a component of the nuclear momentum (the direction of this component is called the hopping vector). In many cases, though, the algorithm may call for a hop that is not allowed by conservation of energy or momentum. Such a hop is called a frustrated hop, and in general frustrated hops cause the number of trajectories propagating on each surface to become inconsistent with the electronic density matrix. Although the fewest switches with time uncertainty (FSTU) method³¹ and the later FSTUVV method³³ have been reasonably successful at producing accurate results despite these difficulties, they occasionally show a strong dependence on the representation used (adiabatic or diabatic), and even when the empirically best representation is used they have been found to be less accurate than the best of the SCP methods described below.

The SE method involves mean-field trajectories, and it can sometimes produce accurate electronic transition probabilities. However, the SE method (even if or when it gives accurate average results) cannot, in general, give accurate final energy distributions because the electronic and translational energies of each trajectory correspond to average energies, whereas the correct physical observables, due to decoherence, correspond to a statistical mixture of the discrete, allowed final values. In a semiclassical method where quantum mechanics is used for the electronic motion and classical mechanics is used for the nuclear motion, the electronic density matrix decoheres due to the “bath” of nuclear coordinates (even for small, isolated, gas-phase systems). The realization that this effect must be introduced explicitly into the SE equation is the motivation for the development of the decay of mixing (DM) methods. To include this decoherence into the mean field approaches, the first DM method, called the natural decay of mixing (NDM) method,¹⁸ replaced the mean-field state with a decohering one by adding decay into the coupled-states electronic Schrödinger equation. A DM trajectory behaves like the mean-field trajectory when the system is in a region of strongly interacting electronic states, but it gradually decoheres into a single-state trajectory when the system leaves the strong interaction region.^{15,16,18} As decoherence is built into the quantum electronic motion, it naturally induces an extra force acting back on the classical nuclear motion. This

force is called the decoherent force, and its magnitude is determined by the requirement of energy conservation. The DM formalism has been shown to provide a more accurate description of non-Born-Oppenheimer dynamics than either the SE or the surface-hopping formalism.^{15,16,18}

The state to which the decohering state is locally decaying is called the decoherent state. This could be an adiabatic or diabatic state; the basis in which physical decoherence occurs is called the pointer basis⁴⁹ or the environmentally induced superselection basis.⁵⁰ Instead of describing nonadiabatic transitions as trajectories hopping discontinuously and stochastically from one potential energy surface to another, as in trajectory surface hopping methods, DM trajectories evolve continuously on a weighted average of the potential energy surfaces, with continuously evolving weights that tend to unity on one surface (in the adiabatic or diabatic basis) and zero on all the others. The decoherent state, rather than the propagation surface, is switched.^{15,16,18} The result is similar to allowing nonvertical hops. The NDM method¹⁸ was the first implementation of the DM formalism, and in the NDM method the switching occurs stochastically according to the TFS algorithm using the decohering electronic density. This was shown to be more accurate than the TFS surface hopping method. The NDM approach has nevertheless been further improved as described below.

In the original formulation of the NDM method, the switching probability artificially favors decoherence to the local decoherent state. This means that the system either decoheres too fast or the switching probability balances coherence with decoherence inappropriately. With this problem in mind, we developed the self-consistent decay of mixing (SCDM) method¹⁵ in which we do not consider the contribution to population transfer due to decay when we compute the switching probabilities. This improves accuracy of the DM method.

Subsequent analysis led to an even more accurate DM method in which the switching probability is governed by the coherent part of the coupled-states electronic Schrödinger equation over each pass through a strong interaction region. Globally coherent switching (i.e., coherent switching over the entire trajectory) is, however, not the best algorithm for simulating full quantum dynamics. The importance of decoherence between successive passages through strong interaction regions was demonstrated most clearly by Thachuk et al.⁴² in a low-dimensionality problem, namely the evolution of a two-state diatomic molecule in a strong electromagnetic field; their discussion makes it clear that the combination of coherent evolution through a strong interaction region and decoherence between such passages is a more realistic model of quantum dynamics than is completely coherent dynamics and that maintaining coherence over an entire trajectory may lead to significant errors. One semiclassical method that was developed with this kind of consideration as a motivation is the surface hopping method of Parlant and Gislason,^{22,23} in which each strong interaction region is treated coherently, and then electronic wave functions are reinitialized before encountering the next strong interaction region. This method, like all TSH methods, models one aspect of decoherence by the hopping events

themselves. However, our tests of the Parlant–Gislason TSH method showed¹⁶ that it is less accurate than the fewest-switches TSH method. We used a similar but different strategy to incorporate decoherence between strong-interaction regions and coherence within strong-interaction regions in the DM method. In particular, we modified the DM method to calculate switching probabilities using fully coherent electronic wave functions, and we reset the coherent wave functions to the decohering ones between strong-interaction regions (rather than reinitializing them). We call this method the coherent switching decay of the mixing (CSDM) method, and we found that it is more accurate than SCDM and NDM.¹⁶

The three methods (NDM, SCDM, and CSDM) differ only in how the decoherent state evolves during the trajectory. Trajectories evolve continuously in all DM methods, and there is no frustrated switching. When a DM trajectory attempts to decohere to an energetically forbidden state, the decoherence slows down, and the trajectory then evolves coherently in a mixed state until the forbidden state becomes allowed or until the dynamics changes in some other way, i.e., though the trajectory cannot fully occupy an energetically forbidden state, it may evolve on an average potential that contains some character of the forbidden state. This differs from TSH methods, where forbidden hops cause the distribution of TSH trajectories to no longer match the distribution called for by the electronic density matrix.

All of the DM methods mentioned so far involve nonlinear decay of mixing of the density matrix because of the way that we originally introduced the decay terms in terms of the wave function; in particular, the off-diagonal terms contain one density matrix element divided by another. From now on, we call these DM methods nonlinear decay of mixing method (NLDM) methods. The key goal of the present paper is to test the sensitivity to recasting the decay of mixing in a linear form, as postulated by most methods cast originally in density matrix language.

Quantum simulation can have two different meanings. It can mean the use of quantum mechanics to simulate physical systems, or it can mean the use of semiclassical algorithms or macroscopic models to simulate quantum systems. We are interested in the latter.

A quantum system interacts with its environment, which destroys the coherence in a robust basis,^{51,52} called the pointer basis or the einselected (environmentally induced superselected) basis.^{52,53} The system decoheres to a statistical classical mixture. We simulate this as stochastic demixing to an ensemble of classical states. The essence of decoherence is finding the robust basis in which the density matrix becomes diagonal; the density matrix is always diagonal in some basis (since it is a Hermitian operator, it has eigenvectors), but only in the pointer basis does it remain diagonal.⁵³

Decoherence is an essential part of any quantum subsystem in contact with an environment, i.e., of any system smaller than the entire universe, and its implications have a profound effect on emergence of applicability of classical modes of thought to quantum systems, that is of classical mechanics as a good approximation to quantum mechanics under certain circumstances.⁵⁰ However, much less attention has been paid

to its relevance for quantum simulation, that is, practical classical-like approximations to quantum systems under conditions where classical mechanics is not applicable and quantum effects are large.⁵⁴

Although more general formulations are available,⁵⁵ considerable attention has been paid to the evolution of a quantum system interacting linearly and perturbatively with a high-temperature thermal environment.^{50,56} However, these assumptions are not always applicable; decoherence is more general, and in some cases we want to concentrate on the more general features of decoherence and the properties it has even when the system-environment interaction is nonlinear, strong, and nonthermal, and when the environmental relaxation time is not fast compared to the primary system dynamical time scale. As an example of a more general property of decoherence, Zurek has pointed out that in general the decoherence rate cannot be faster than the inverse of the spectral cutoff of the environment or the rate at which coherence is created.⁵⁰ An example of a general feature that might be relevant for our work here is that if the environment is more classical than the system, decoherence should be rapid compared to relaxation. For example, if vibronic relaxation occurs on the picosecond time scale, decoherence might be much faster, for example, faster than a tenth of a picosecond.

The approach to the quantum simulation embodied in the decay of mixing methods is to replace the Liouville-von Neumann (LvN) equation, which is equivalent to the Schrödinger equation and describes the “apparent ensemble”⁵⁷ corresponding to a pure superposition state, by a fictitious, stochastic ensemble evolving according to a modified LvN equation containing relaxation terms. To emphasize the distinction, the original LvN equation may be called the unitary LvN equation, and the modified one may be called a quantum master equation. The use of stochastic ensembles has a long history in the quantum theory of open systems,⁵⁸ and the decay of mixing methods involves using the concept to create new semiclassical algorithms. We will see that some old questions appear in new guises. For example, “What is the pointer basis?” becomes “Is the adiabatic or diabatic representation a closer approximation to the true pointer basis in the interaction region?” or even “Since the true pointer basis in the interaction region is unknown, can we devise an algorithm whose accuracy does not depend strongly on the choice of representation?”. Similarly, the question “What is the physical decoherence rate?” becomes “What algorithmic decoherence rate allows the observables calculated from an ensemble of semiclassical trajectories to best simulate the observables calculated from a quantum wave packet?”.

Note that we have used the term “quantum master equation” rather than “dissipative LvN equation”—either can be used in this context. It is important though to keep in mind that “dissipation” often refers to essentially irreversible transfer of energy into a subsystem with many degrees of freedom, where it is lost; and the decoherence that has been most heavily discussed involves transfer of information into a many-degrees-of-freedom subsystem where it is lost. Even “relaxation” sometimes has the connotation of interaction

with a heat bath. In contrast, consistent with recent appreciations of the broader context in which decoherence must be studied,⁵⁹ here we consider a small environment, the nuclear degrees of freedom of a gas-phase molecule. Furthermore, whereas the goal of much master equation work is to eliminate the need to treat the environmental system explicitly, in the present work we treat the environment explicitly, but because we make a classical approximation for the environment, we need to introduce decoherence explicitly into the quantum primary system. A question we have asked in previous work is as follows: Can we formulate stochastic demixing of the primary system (the electronic degrees of freedom) to an ensemble of noninterfering states by adding relaxation terms (a time-asymmetric mechanism) to a Schrödinger equation and transforming to the density matrix language (as has been done in the decay of mixing methods)? In the present article we follow this with the following: How does this compare to adding relaxation terms directly to the LvN equation, as is usually done? Is there an essential reason to prefer one or another of these methods for formulating a statistical, irreversible, local equation of motion that describes a subsystem (the electronic degrees of freedom) strongly coupled to an environment (the nuclear degrees of freedom)?

Master equations (equations, usually approximate, for the evolution of a density matrix or the diagonal elements of a density matrix) may be classified as Markovian (time local, generated by a positive semigroup of irreversible time evolution⁶⁰) or non-Markovian.^{54,55,61,62} We have used both approaches: the natural switching and self-consistent switching methods are Markovian, whereas our more recent coherent switching method is non-Markovian, and the time nonlocality (memory) is controlled by an auxiliary density matrix and a strong-interaction criterion that controls the time interval over which the auxiliary density matrix is propagated coherently. One of the attractive features of the coherent switching decay of the mixing method is that although it describes non-Markovian evolution, it does so entirely in terms of differential equations, without the requirement for integrodifferential equations, a feature that has also occurred in some earlier work.⁶¹ We will see that the various elements may, in principle, be combined in more than one way, and one of the goals of the present paper is to test the robustness of the resulting semiclassical methods to changing these elements.

Although the NLDM schemes were originally developed by adding decay terms to the time-evolution of the electronic wave function, i.e., to the time-dependent Schrödinger equation,¹⁸ the Schrödinger equation of motion including these decay terms may be transformed into a Liouville-von Neumann equation.^{15,16} Although these equations of motion are theoretically equivalent, it is easier to reformulate the DM methods in a linear way if one works directly with the density matrix, and this is accomplished in section II. Section III presents various switching algorithms for decoherent states in this context. Section IV reviews the decay time and the decoherent direction. Section V presents several computational details. Section VI tests several semiclassical methods, involving both linear and nonlinear decay of mixing with decoherent and coherent switching, for 17 test cases involv-

ing 8 three-dimensional atom–diatom systems. Section VII presents concluding remarks.

II. Decay of Mixing Methods

In this section, we present the theory entirely in terms of the density matrix without referring to the equations of motion for the wave function. In the decay of mixing methods, the time derivative of the density matrix has two components: one arising as the solution to the fully coherent Liouville-von Neumann equation and one that incorporates electronic decoherence. In general, we write¹⁶

$$\dot{\rho}_{kk'} = \dot{\rho}_{kk'}^C + \dot{\rho}_{kk'}^D \quad (1)$$

where the coherent part is given in a general representation (diabatic or adiabatic) by

$$i\hbar\dot{\rho}_{kk'}^C = \sum_l ([U_{kl} - i\hbar\dot{\mathbf{R}} \cdot \mathbf{d}_{kl}]\rho_{lk'} - \rho_{kl}[U_{lk'} - i\hbar\dot{\mathbf{R}} \cdot \mathbf{d}_{lk'}]) \quad (2)$$

where k, k' , and l label electronic states ($k, k', l = 1, 2, \dots, m$, where m is the number of electronic states), \mathbf{R} is an N -dimensional vector of nuclear coordinates, an overdot denotes a time derivative, and $U_{kk'}$ is the symmetric potential energy matrix defined by

$$U_{kk'} = \langle k | H_{\text{el}} | k' \rangle \quad (3)$$

where H_{el} is the electronic Hamiltonian plus nuclear repulsion. The nonadiabatic coupling vector $\mathbf{d}_{kk'}$ is an $m \times m$ anti-Hermitian matrix in electronic state space, and each element is a vector in \mathbf{R}

$$\mathbf{d}_{kk'} = \langle k | \nabla_{\mathbf{R}} | k' \rangle \quad (4)$$

where $\nabla_{\mathbf{R}}$ is the N -dimensional nuclear gradient. In the adiabatic representation, \mathbf{U} is a diagonal matrix called \mathbf{V} ; and one can define a “diabatic” representation where $\mathbf{d}_{kk'}$ is zero and \mathbf{U} is not diagonal (although true diabatic representations do not exist,⁶³ approximate diabatic representations^{63–66} are very useful and are widely used in approximations). The second term of eq 1 is an algorithmic control term added to simulate decoherence.

By conservation of density

$$\sum_{k=1}^m \dot{\rho}_{kk} = 0 \quad (5)$$

and eq 2 leads to conservation for the coherent terms

$$\sum_{k=1}^m \dot{\rho}_{kk}^C = 0 \quad (6)$$

thus we obtain a restriction on the decay terms:

$$\sum_{k=1}^m \dot{\rho}_{kk}^D = 0 \quad (7)$$

Clearly $\dot{\rho}_{kk}$, $\dot{\rho}_{kk}^C$, and $\dot{\rho}_{kk}^D$ can be either negative or positive. Whereas $\dot{\rho}_{kk}^C$ is determined by the time-dependent Schrödinger equation, $\dot{\rho}_{kk}^D$ results from algorithmic choice. We formulate the DM methods such that there is some electronic

state K (the “decoherent state”) toward which the system is decohering, and this requires that $\dot{\rho}_{kk}^D < 0$ for $k \neq K$ and $\dot{\rho}_{KK}^D > 0$. This guarantees that the trajectory corresponds asymptotically to a particular electronic state in the pointer basis. Assuming that the diagonal elements decay by a linear, first-order process yields

$$\dot{\rho}_{kk}^D = -\frac{1}{\tau_{kK}}\rho_{kk}, \quad k \neq K \quad (8)$$

and

$$\dot{\rho}_{KK}^D = \sum_{k \neq K} \frac{1}{\tau_{kK}}\rho_{kk} \quad (9)$$

where τ_{kK} is a first-order decay time to be specified. The time derivatives $\dot{\rho}_{kk}^D$ of the off-diagonal matrix elements are not yet specified, and they are discussed later.

The introduction of the decay term of eq 8 is the key element of the decay-of-mixing methods. In a real physical situation, a system interacting with an environment ends in a mixed state, rather than a pure state, which would result if the density matrix, originally assumed pure, were evolved by the time-dependent Schrödinger equation. We want to simulate the final ensemble corresponding to the mixed state of the electronic subsystem by an ensemble of pure states. Thus, whereas the destruction of interference in the real system leads to a mixture that corresponds to a probability distribution of final observables, the simulation system tends to a probabilistic distribution of pure states, each corresponding to different observables.

Next, we consider the nuclear motion. We use an iso-inertial, mass-scaled nuclear coordinate system \mathbf{R} in which all nuclear masses are scaled to the same reduced mass μ , and the momentum conjugate to \mathbf{R} is called \mathbf{P} . The nuclear motion is represented by an ensemble of classical trajectories, and the nuclear position and momentum of each trajectory evolve according to classical equations of motion

$$\dot{\mathbf{R}} = \mathbf{P}/\mu \quad (10)$$

and

$$\dot{\mathbf{P}} = \dot{\mathbf{P}}^C + \dot{\mathbf{P}}^D \quad (11)$$

where the coherent part is^{15,16}

$$\dot{\mathbf{P}}^C(t) = -\sum_k \rho_{kk} \nabla_{\mathbf{R}} U_{kk} - \sum_k \sum_{k' < k} (2\text{Re}\rho_{kk'}) \nabla_{\mathbf{R}} U_{kk'} + \sum_j \sum_k \sum_{k' < k} (2\text{Re}\rho_{kj}) U_{kk'} \mathbf{d}_{kj} \quad (12)$$

and the decoherent part is^{15,16,18}

$$\dot{\mathbf{P}}^D = -\frac{\mu \dot{V}^D}{\mathbf{P} \cdot \hat{\mathbf{s}}} \hat{\mathbf{s}} \quad (13)$$

where^{15,16}

$$\dot{V}^D = \sum_k \dot{\rho}_{kk}^D U_{kk} + \sum_k \sum_{k' < k} 2\text{Re}(\dot{\rho}_{kk'}^D) U_{kk'} \quad (14)$$

and $\hat{\mathbf{s}}$ is a unit vector (specified below) that represents the decoherence direction into which energy is deposited and

out of which energy is consumed. The right-hand side of eq 13 is the negative of the decoherent force, and it drives the trajectory to a pure electronic state. The decay of mixing methods differ in the off-diagonal matrix elements $\dot{\rho}_{kk'}^D$, as discussed next.

A. Nonlinear Decay of Mixing (NLDM). Previously, we added first-order decay to the electronic wave function.^{15,16,18} By making the reasonable assumption¹⁸ that the real and imaginary parts of the component of the electronic wave function corresponding to a given electronic state decay at the same rate (in a particular representation, i.e., in the pointer basis), we obtained equations which are equivalent to the following decay law for the decoherence in the pointer representation^{15,16}

$$\dot{\rho}_{ij}^D = \begin{cases} -\frac{1}{2} \left(\frac{1}{\tau_{iK}} + \frac{1}{\tau_{jK}} \right) \rho_{ij} & i \neq K, j \neq K \\ \frac{1}{2} \left(\frac{1}{\rho_{KK}} \left(\sum_{k \neq K} \frac{\rho_{kk}}{\tau_{Kk}} \right) - \frac{1}{\tau_{jK}} \right) \rho_{ij} & i = K, j \neq K \\ \frac{1}{2} \left(\frac{1}{\rho_{KK}} \left(\sum_{k \neq K} \frac{\rho_{kk}}{\tau_{Kk}} \right) - \frac{1}{\tau_{iK}} \right) \rho_{ij} & i \neq K, j = K \end{cases} \quad (15a)$$

$$\dot{\rho}_{ij}^D = \begin{cases} \frac{1}{2} \left(\frac{1}{\rho_{KK}} \left(\sum_{k \neq K} \frac{\rho_{kk}}{\tau_{Kk}} \right) - \frac{1}{\tau_{jK}} \right) \rho_{ij} & i = K, j \neq K \end{cases} \quad (15b)$$

$$\dot{\rho}_{ij}^D = \begin{cases} \frac{1}{2} \left(\frac{1}{\rho_{KK}} \left(\sum_{k \neq K} \frac{\rho_{kk}}{\tau_{Kk}} \right) - \frac{1}{\tau_{iK}} \right) \rho_{ij} & i \neq K, j = K \end{cases} \quad (15c)$$

where the decay terms for the diagonal elements push ρ_{KK} in the denominator to unity and ρ_{kk} in the summation to zero. The nonlinear terms in eq 15 therefore vanish asymptotically.

B. Linear Decay of Mixing (LDM). We linearize the decay of mixing by ignoring nonlinear terms in eq 15. Then we have

$$\dot{\rho}_{kk'}^D = -\frac{1}{2\tau_{kk'}} \rho_{kk'}, k \neq k' \quad (16)$$

where the factor of 2 in eq 16 is not necessary, and we could put any nonzero constant there; however, here we define the decay time to be consistent with notation used above. The decay times in eq 16 need not be the same as those that appear in the diagonal matrix elements in eqs 8 and 9, but in the present article we take them to be the same for simplicity.

Equations 15a and 16 lead to the widely assumed situation where coherence decays exponentially. This form for the decay can be derived under reasonable sets of assumptions for other problems,⁶⁷ but for the present problem of the decoherence of the electronic degrees of freedom by the nuclear ones, it has the status of a possible fundamental assumption.

C. Population-Driven Decay of Mixing (PDDM). In the population-driven decay of mixing (PDDM) method, we assume that there is no decoherent decay of the off-diagonal matrix, i.e.

$$\dot{\rho}_{kk'}^D = 0, k \neq k' \quad (17)$$

Note that this method, like LDM, is linear. If we use the usual convention that the relaxation time for the diagonal elements is called T_1 and that for the off-diagonal elements is called T_2 , this corresponds to $T_2 = \infty$ and T_1 finite, whereas

usually $T_2 \leq T_1$. However, we should keep in mind that the decoherent decay in the DM methods is algorithmic decay, not physical decay. We are adding decay terms to the equations for an ensemble of independent semiclassical trajectories so that the ensemble average best simulates the behavior of a quantum wave packet. In this case, it is interesting to test the effect of making a minimal perturbation to the equations of motion consistent with forcing the system to continuously switch to a single potential energy surface asymptotically. In the PDDM scheme, we make only this minimal perturbation.

Note that $\rho_{kk'}$ for $k \neq k'$ does not tend to zero in this method, just as it also stays finite in trajectory surface hopping. However, as compared to trajectory surface hopping, the system has no discontinuous changes in momenta, and it uses Ehrenfest-like dynamics in regions where the potential energy surfaces are strongly coupled. Thus the PDDM method provides an algorithmic density matrix that may be useful for calculations, but it does not necessarily satisfy the constraint⁸

$$\rho_{nn}\rho_{mm} \geq |\rho_{nm}|^2$$

which holds for true density matrices.

III. Decoherent and Coherent Switching

Next we discuss how the decoherent state is switched along the DM trajectory. In the TSH method, at a hop, the trajectory discontinuously switches from one pure electronic state to another pure electronic state. In DM methods we instead switch the decoherent state.

A. Natural Switching (NS). The natural switching (NS) scheme is a direct application of Tully's fewest-switches scheme. For example, in the two-state case, the probability of switching from a decoherent state K to some other decoherent state K' between time t and time $t + dt$ is given by

$$P_{K \rightarrow K'} = \max \left(-\frac{\dot{\rho}_{KK} dt}{\rho_{KK}}, 0 \right) = \max \left(-\frac{(\dot{\rho}_{KK}^C + \dot{\rho}_{KK}^D) dt}{\rho_{KK}}, 0 \right) \quad (18)$$

The multistate generalization of eq 18 is given in Appendix A of ref 16.

B. Self-Consistent Switching (SCS). In eq 18 above, the change in the density matrix elements, including the change due to decoherence, is used to calculate the switching probability. In the self-consistent switching (SCS) scheme, the switching probability is calculated using only the coherent part of the change in elements of the density matrix. In the two-state case this yields

$$P_{K \rightarrow K'} = \max \left(-\frac{\dot{\rho}_{KK}^C dt}{\rho_{KK}}, 0 \right) \quad (19)$$

This may be interpreted as "semicoherent switching" because the instantaneous change in the density matrix due to decoherence is not included, although the decoherence due to the trajectory's history is included in the denominator of

eq 19, since ρ_{KK} is the decohered density. The multistate generalization of eq 19 is given in Appendix A of ref 16.

C. Globally Coherent Switching (GCS). The globally coherent switching (GCS) method preserves coherence in the populations used to control switching over the entire trajectory. To accomplish this, we define a set of coherent state populations $\tilde{\rho}_{KK'}$ which satisfy the fully coherent evolution given in eq 2. Initially $\tilde{\rho}_{kk'} = \rho_{kk'}$, but these two density matrices are propagated separately. In the two-state case the switching probability is given by

$$P_{K \rightarrow K'} = \max\left(-\frac{\tilde{\rho}_{KK} dt}{\tilde{\rho}_{KK}}, 0\right) \quad (20)$$

D. Coherent Switching (CS). The above schemes are all time-local (or Markovian), but the actual time derivatives of the density matrix are not only solely determined by information about the current state of the system but also by its time history, i.e., the evolution is nonlocal in time or non-Markovian. In this section we discuss a key feature that accounts for such time nonlocality, and we show how to include a critical aspect of memory into the propagation by incorporating the concept of a localized (but not instantaneous) interaction between the quantum states.

Parlant and Gislason³ introduced a method in the framework of trajectory surface hopping (TSH) that we called exact coherent passage TSH (ECP-TSH). In this method (for a two-state case) the following coupling function is monitored:

$$\Omega(t) = |\dot{\mathbf{R}} \cdot \mathbf{d}_{12}(t)| \quad (21)$$

At each local minimum of Ω , the density matrix is reinitialized to correspond to a pure state, i.e., $\rho_{KK} = 1$ and all other elements equal zero. The ECP-TSH method integrates the electronic equations of motion in a coherent way throughout each complete transversal of a strong coupling region, but it handles decoherence differently from the DM methods in several respects. First, there is no decay of mixing term. Second, each trajectory propagates locally on a single potential surface rather than an Ehrenfest-weighted surface. Third, the ECP-TSH method involves hops with discontinuities in the nuclear momentum, and when a hop occurs it requires that the semiclassical trajectory be repropagated from a point of maximal coupling. Fourth, whether a hop occurs, at each local minimum of $\Omega(t)$, the electronic coefficients are reinitialized to unity or zero. This means that decoherence is instantaneous in the ECP-TSH method, and it appears from the results¹⁶ that this does not describe decoherence as well as possible. Nevertheless, this idea provided stimulation for a (locally) coherent switching scheme that we abbreviate CS.

In the CS scheme, the switching probability is defined as in eq 20 for the GCS method. In the CS scheme however, $\tilde{\rho}_{KK'}$ is set equal to $\rho_{KK'}$ at all local minima of some coupling function. *Note that we sync the switch-controlling density matrix to the decohered one (that controls the effective potential) rather than reinitialize it.* By setting $\tilde{\rho}_{KK'} = \rho_{KK'}$, the amount of decoherence is determined by the difference between the two sets of electronic density matrices: the one that is propagated with decay-of-mixing terms and the one that is propagated coherently. Thus, in particular, the amount

of decoherence introduced at a local minimum of the coupling function depends on the size of the coupling region and other dynamical factors. We emphasize that the equations of motion governing the $\tilde{\rho}_{ij}$ elements and hence governing the switching probability in the CS method are treated in a coherent and uninterrupted way throughout each complete passage through a strong coupling region (although one does allow switches in the decoherent state), but decoherence is introduced into $\tilde{\rho}_{ij}$ between different strong coupling regions by setting $\tilde{\rho}_{ij} = \rho_{ij}$ at minima of the coupling function.

We have not used the same coupling function as Parlant and Gislason. We previously defined the following functions for both adiabatic and diabatic representations¹⁶

$$D_K(t) = \sum_j |\mathbf{d}_{Kj}|^2 \quad (22)$$

and

$$C_K(t) = \sum_j |\mathbf{d}_{Kj} \cdot \dot{\mathbf{R}}_{\text{vib}}|^2 \quad (23)$$

Calculations employing eq 22 are called CS, and those employing eq 23 are called CS-C. These coupling functions arise from the adiabatic representation where the coupling is determined by the nonadiabatic coupling vector, but it is clear (at least for the two-state case) that they also provide a measure of coupling in the diabatic representation. Nevertheless, it is interesting to ask if a quantity computed directly in the diabatic representation works as well. Thus we define

$$S_K(t) = \sum_{j \neq K} |U_{Kj}|^2 \quad (24)$$

and

$$L_K(t) = \sum_j |U_{KK} - U_{jj}|^2 \quad (25)$$

The first quantity, eq 24, is a direct expression in terms of the scalar-coupling (S) matrix elements, and the second, eq 25, is a measure of deviation from the crossing point where a local minimum (which might be zero) occurs in the diabatic level-spacing (L). We also consider using the reciprocal of eq 25. Equations 22, 24, and 25 and the reciprocal of 25 will be considered as alternative demarcation schemes for strong-coupling regions in CS calculations. Note that these four equations give qualitatively different definitions of a strong-coupling region for many problems.

When it is desired to associate a unique abbreviation with each choice, calculations carried out using eq 22 may be labeled CS(D), that is, coherent switching based on the magnitude of the derivative coupling; those with eq 23 may be labeled CS-C, that is, coherent switching with strong interaction boundaries based on a component; those carried out with eq 24 may be labeled CS(S), that is, coherent switching with strong-interaction boundaries based on scalar diabatic coupling; those carried out with eq 25 may be labeled CS(L), that is, coherent switching in the diabatic representation with strong-interaction boundaries based on diabatic level-spacing; and those carried out with the

reciprocal of (25) will be labeled CS(1/L). A possible advantage of choosing the S, L, or 1/L expressions in the diabatic representation is that one can avoid the diabatic–adiabatic transformation. This may be useful for some systems, although in general, given a diabatic representation, this transformation is not computationally demanding. Thus the motivation for choosing a particular demarcation scheme will be the consistency of the semiclassical formulation, as judged by the accuracy of the results for a diverse set of problems.

E. Combinations. We have defined five switching schemes (natural switching, self-consistent switching, globally coherent switching, coherent switching basis on a component, and coherent switching) in the adiabatic representation. Any of these schemes may be used in combination with the three decay of mixing algorithms (NLDM, LDM, and PDDM) discussed in section II for a total of 15 semiclassical methods in the adiabatic representation. In the diabatic representation we will consider the D, S, L, and 1/L criteria for strong-interaction regions in the CS scheme, for a total of eight schemes and 24 combinations. However some of these are only of academic interest at this point since we know from previous work^{15,16} that the NS, SCS, and CS-C schemes are less accurate than CS. But the GCS, CS(S), CS(L), and CS-(1/L) schemes have never been tested. Some of the combinations are equivalent to previous methods: NLDM with NS is NDM; NLDM with SCS is SCDM; NLDM with CS-C is CSDM-C; and NLDM with CS is CSDM. The other 20 are new. To emphasize the essential characteristics, LDM with CS is abbreviated CSDM/L, and PDDM with CS is abbreviated CSDM/PD. Furthermore, NLDM, LDM, and PPDM with GCS may be abbreviated GCSDM, GCSDM/L, and GCSDM/PP, respectively.

IV. Decay Time and Decoherence Direction

Next we review how the decay time and decoherent direction are determined. The same prescriptions¹⁶ are used for all of the combinations, and they are summarized briefly here to make this paper more self-contained.

The unit vector in eq 13 represents the direction into which nuclear kinetic energy is deposited or out of which energy is consumed, and in the two-state case it is given by¹⁶

$$\hat{\mathbf{s}} = (d_{KK}a_0(\mathbf{P} \cdot \hat{\mathbf{d}}_{KK})\mathbf{d}_{\hat{K}K} + P_{\text{vib}}\hat{\mathbf{P}}_{\text{vib}})/\|\mathbf{d}_{KK}a_0(\mathbf{P} \cdot \hat{\mathbf{d}}_{KK})\mathbf{d}_{\hat{K}K} + P_{\text{vib}}\hat{\mathbf{P}}_{\text{vib}}\| \quad (26)$$

where a_0 is a bohr length, $\hat{\mathbf{P}}_{\text{vib}}$ and $\hat{\mathbf{d}}_{KK}$ are unitless unit vectors in the direction of \mathbf{P}_{vib} (the local vibrational momentum²⁶) and \mathbf{d}_{KK} , respectively, and d_{KK} is the magnitude of \mathbf{d}_{KK} . The generalization of eq 26 to multiple states has been given previously.^{15,16}

The decay time we use is¹⁶

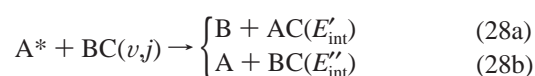
$$\tau_{kK} = \frac{\hbar}{|V_{kk} - V_{KK}|} \left(1 + \frac{E_0}{(\mathbf{P} \cdot \hat{\mathbf{s}})^2 / 2\mu} \right) \quad (27)$$

where E_0 is a constant. In the present work we use $E_0 = 0.1 E_h$ (where $1 E_h \equiv 1 \text{ hartree} = 27.2116 \text{ eV}$), which is the same value as used in ref 16.

Equation 27 exhibits two very interesting qualitative features. First, individual off-diagonal density matrix elements do not all decohere at the same rate, and coherences between levels that are widely separated decay faster than those between levels that are close to each other. This behavior has been observed in semiclassical studies of an oscillator coupled to a bath.^{68,69} Second, the decoherence time tends to ∞ as the momentum tends to zero. This feature, which follows in our work from the self-consistent treatment of the system–environment interaction, is consistent with a study⁷⁰ based on a general master equation that showed that coherence decay becomes slower than any exponential as the environmental temperature tends to zero.

V. Three-Dimensional, Two-State Test Cases

The model systems we consider here are two-state atom–diatom nonadiabatic collisions and have the form



where A, B, and C label atoms, the asterisk indicates electronic excitation, and ν and j are the initial vibrational and rotational quantum numbers. Equation 28a describes the nonadiabatic reaction, where E'_{int} is the final internal (i.e., rovibrational) energy of the AC diatom, and eq 28b describes quenching, where E''_{int} is the final internal energy of the BC diatom. We label the initial conditions by the total energy E and the initial vibrational and rotational quantum numbers ν and j of the diatomic molecule. For all of the cases considered here, the total angular momentum of the system is zero. Electronic angular momentum is neglected consistently in both the quantal and semiclassical calculations.

For the collision energies used in this paper, there are only three possible collision outcomes (combinations of the final arrangement and electronic state): adiabatic collision in the electronically excited state, reactive de-excitation, and quenching (nonreactive de-excitation).

The semiclassical trajectory calculations and the accurate quantum mechanical results are compared for the following six quantities ($i = 1, 2, \dots, 6$): P_R , the probability of reaction, which is the outcome in eq 28a; P_Q , the probability of quenching, which is the outcome in eq 28b; P_N , the total probability of a nonadiabatic event, which is the sum of P_R and P_Q ; F_R , the reactive branching fraction, which is defined as P_R/P_N ; $\langle E'_{\text{int}} \rangle$, the average internal (vibrational–rotational) energy of the diatomic fragment in eq 28a; and $\langle E''_{\text{int}} \rangle$, the average internal (vibrational–rotational) energy of the diatomic fragment in eq 28b. For the three probabilities the error $\epsilon_{i\alpha}$ for quantity i and test case α (nine cases for MXH, five cases for MCH, and three case for YRH) is calculated as the logarithmically averaged percentage error computed as described elsewhere,⁷¹ and for the remaining three quantities, F_R , $\langle E'_{\text{int}} \rangle$, and $\langle E''_{\text{int}} \rangle$, the error $\epsilon_{i\alpha}$ is defined as the unsigned relative percentage error computed as described elsewhere.¹⁶ The average of the logarithmically averaged percentage errors in P_R , P_Q , and P_N is called the average unsigned percentage error in probabilities (column heading “Prob”), and the average of the unsigned relative

percentage errors in F_R , $\langle E'_{\text{int}} \rangle$, and $\langle E''_{\text{int}} \rangle$ is called the average unsigned percentage error in fractional distributions (column heading “Fract”); the latter name is appropriate because the relative error in internal energy is identical to the relative error in the fraction of total energy that is deposited in internal energy. Finally, we average the two averages to obtain an average unsigned percentage error for all six observables (column heading “All”).

The model systems feature three types of nonadiabatic transitions and are labeled as MXH, MCH, or YRH.

The MXH systems feature avoided crossings of the Landau–Zener type^{72–74} in which the two diabatic potential energy surfaces cross with nonzero diabatic coupling. Nine MXH cases are included: the SB, SL, and WL parametrizations, with total energy $E = 1.1$ eV, $\nu = 0$, and $j = 0, 1, 2$. Details of the MXH parametrizations and the accurate quantum mechanical calculations have been given previously.⁴⁷ For the MXH systems, the quantum transition probabilities show oscillations, but the semiclassical methods do not. Therefore, for MXH systems, semiclassical results for P_R , P_Q , P_N , and F_R at 1.1 eV are compared to quantal results averaged over an energy interval. When a quantity, say α , is quantum mechanically averaged at E_0 , it means

$$\bar{\alpha}(E_0) = \frac{1}{2N+1} \sum_{j=-N}^N \alpha(E_0 - j\delta E) \quad (29)$$

where δE is small increment around E_0 . In applying eq 29 to the MXH systems in the present paper, N is 2 and $\delta E = 0.0055$ eV. The values of $\langle E'_{\text{int}} \rangle$ and $\langle E''_{\text{int}} \rangle$ are not averaged.

The MCH systems feature conical intersections^{75–77} in which the two diabatic potential energy surfaces cross at some geometries where the diabatic coupling is zero. Five MCH cases are included: the SB, SL, TL, WB, and WL parametrizations, with $E = 1.1$ eV and $\nu = j = 0$. Details of the MCH parametrizations and the accurate quantum mechanical calculations have been given previously.⁷⁸ For MCH and YRH systems, the quantal results used for comparison in this article are not averaged.

The YRH systems feature interactions of the Rosen-Zener-Demkov type,^{79–81} by which we mean cases where the two diabatic potential energy surfaces do not cross and are weakly coupled. Three YRH cases are included: the YRH(0.1) parametrization with $E = 1.1$ eV and $\nu = j = 0$ and the YRH(0.2) parametrization with $E = 1.02$ eV and $\nu = j = 0$ and $E = 1.1$ eV, $\nu = 0$, and $j = 6$. The number in parentheses denotes the strength of the coupling; this and other details of the YRH parametrizations and the accurate quantum mechanical calculations have been given previously.⁸²

For the decay of mixing trajectories, the coordinates and momenta of the nuclei and the electronic state populations are integrated using an adaptive integration algorithm that was designed for use with semiclassical trajectory calculations.²⁸ The algorithm uses a Bulirsch-Stoer integrator with polynomial extrapolation⁸³ modified such that the integrator is prohibited from stepping over local peaks and minima in the electronic probabilities. For the present calculations, the integration parameters were given the following values:⁴⁷ ϵ_{BS}

$= 10^{-12} E_h$ and $h_{\text{min}} = 10^{-4}$ aut (1 aut = 1 atomic unit of time = 2.4189×10^{-2} fs), which gives converged results for the MXH, MCH, and YRH systems. The trajectories begin the simulation with the lone atom (Y in the case of YRH and M in the case of MXH and MCH) separated from the center-of-mass of the diatom by 35 a_0 (1 $a_0 = 0.52918$ Å) for the MXH, MCH cases and by 20 a_0 for the YRH cases, and the simulation was ended when the product fragments were separated by at least 30 a_0 for all three systems. We have verified that the results of the semiclassical simulations do not change when these distances are increased.

For the decay of mixing trajectories, the final state internal energies, E'_{int} or E''_{int} , are determined without quantization. In particular, the relative translational energy becomes constant after the collision, and the internal energy is computed as total energy minus the final relative translational energy minus the minimum electronic energy of the diatomic fragment.

Calculations are performed in the adiabatic (a) and diabatic (d) representations. Calaveras County (CC) calculations with three combinations of adiabatic and diabatic representations are also performed. The Calaveras County representation⁴⁸ is defined as the representation with the fewest hopping attempts in a trajectory surface hopping calculation, and previous work has shown^{48,77} that this representation is, on average, the most accurate representation for non-Born-Oppenheimer semiclassical trajectory calculations.

All new calculations in this paper were run with the NAT computer code—version 9.0, whereas results in previous papers (some of which are reanalyzed below for the final table) are calculated with the NAT-version 8.1.⁸⁴

VI. Results and Discussion

The Supporting Information provides full sets of calculated observables and average errors for all 15 combinations (see section III.E) in the adiabatic representation and for 18 of the possible combinations in the diabatic representation. In the printed article, that is, in this section, we tabulate and discuss only the most interesting new results.

Table 1 presents the mean percentage errors for the NLDM, LDM, and PDDM methods employing CS switching. The table is based on 17 cases for 10 different systems of three different types, and so it provides a broad assessment of the accuracy and robustness of the methods. The table shows that the YRH systems present the most critical test of which algorithm is the best. All NLDM, LDM, and PDDM methods with CS switching work almost equally well in the adiabatic and Calaveras County representations, but the NLDM and PDDM methods are slightly better than the LDM method in the diabatic representation. The S and L criteria for strong interaction regions appear to work well for diabatic LDM and PDDM calculations. In comparing the results in Table 1 it is not necessary to consider costs since the costs for all methods in the table are within about a factor of 2 or even closer.

The overall results in the last column of Table 1 are obtained by averaging over the three types of system, with each type weighted one-third. The NLDM method with CS switching, which is the CSDM method presented previ-

Table 1. Average Unsigned Percentage Errors Computed for the Coherent Switching Method

method	rep	MXH (avoided crossing)			MCH (conical interaction)			YRH (noncrossing)			all overall ^b
		prob	fract	all ^a	prob	fract	all ^a	prob	fract	all ^a	
NLDM	a	28	20	24	44	24	34	16	17	17	25
	d(D)	21	16	19	34	21	28	43	22	32	26
	d(S)	22	16	19	34	21	27	36	23	29	25
	d(L)	21	16	19	34	21	28	49	26	38	28
	d(1/L)	21	17	19	33	21	27	64	29	47	31
	CC(D)	29	20	24	34	23	29	16	17	17	24
	CC(D,S)	29	20	25	34	23	29	16	17	17	24
	CC(D,L)	29	20	25	34	23	28	16	17	17	23
LDM	a	24	18	21	43	23	33	18	17	18	24
	d(D)	27	20	24	36	21	29	106	15	61	38
	d(S)	27	20	23	34	20	27	53	14	33	28
	d(L)	26	20	23	37	22	29	44	16	30	27
	d(1/L)	27	20	23	34	21	28	51	17	34	28
	CC(D)	28	18	23	35	22	29	18	17	18	23
	CC(D,S)	27	18	23	34	22	28	18	17	18	23
	CC(D,L)	27	18	22	36	23	29	18	17	18	23
PDDM	a	27	20	23	42	22	32	20	16	18	24
	d(D)	26	16	21	37	19	28	78	15	47	32
	d(S)	26	16	21	37	19	28	33	14	24	24
	d(L)	25	16	20	38	20	29	27	16	22	24
	d(1/L)	25	16	20	37	19	28	32	18	25	24
	CC(D)	20	19	25	38	20	29	20	16	18	24
	CC(D,S)	30	19	25	38	20	29	20	16	18	24
	CC(D,L)	29	19	24	38	21	30	20	16	18	24

^a All six observables (average of two previous columns). ^b This column is the average of the three previous "all" columns.

ously,¹⁶ has a mean error of 25% in the adiabatic representation, 26% in the diabatic representation with the original D criterion for strong interaction regions, and 25% in the diabatic representation with the new S criterion. The Calaveras County representation with the D criterion for both representations has 24% error, and using D in the adiabatic representation and S in the diabatic representation gives 23% error. All of these average errors, in the range of 23–26%, are comparable to the kind of error one can get from trajectory calculations for Born-Oppenheimer systems,⁸⁵ so it seems unlikely that further reductions are possible by changing the treatment of nonadiabaticity. Indeed the linearized method, LDM, is slightly worse. Furthermore, decreasing the decoherent algorithmic control to the minimum necessary to guarantee physical final electronic states, as in the PDDM method, gives almost the same overall mean errors, ~24%, as the CSDM, provided one uses either the S or L criterion in the diabatic representation. We conclude that the decay-of-mixing methods are very robust with respect to details of the implementation and that the linearized methods perform equally as well as our wave function version in the adiabatic representation, which gives nonlinear decay of the density matrix. The fact that the PDDM method with the D criterion in the adiabatic approximation and the S criterion in the diabatic approximation are sometimes slightly more accurate than the CSDM method is interesting, but it is outweighed by the more physical character of the CSDM in driving the off-diagonal elements of the density matrix toward zero and by the fact that the overall errors of the CSDM and the PDDM are almost identical.

Although we have emphasized the physicality of the DM methods in driving the coherences (the off-diagonal elements of the density matrix are called coherences in the density matrix literature) to zero, the nonlinear and linearized versions of the method differ in the way that they accomplish this. This is best illustrated by considering the two-state case. For two states, with $k = 1$, $K = 2$, and $\tau_{21} = \tau_{12}$, eq 15 of the CSDM method yields

$$\dot{\rho}_{12}^D = -\left(\frac{\rho_{11}}{\rho_{22}} - 1\right) \frac{\rho_{12}}{2\tau_{12}} \quad (30)$$

whereas eq 16 of the LDM yields

$$\dot{\rho}_{12}^D = -\frac{\rho_{12}}{2\tau_{12}} \quad (31)$$

Equation 31 has the behavior that the decoherent control terms always decrease $|\rho_{12}|$, as assumed by phenomenological theories of decoherence, whereas eq 30 does not have this behavior. However, since we are working with algorithmic demixing rather than physical demixing, and since eq 30 follows from adding a decay mechanism to the wave function equation of motion, one can argue that the requirement that $\dot{\rho}_{12}^D/\rho_{12}$ is negative need not be enforced and might even be inappropriate. In fact, Elran and Brumer,⁶⁹ in a study of an anharmonic oscillator coupled to a bath, found that coherence both increased and decreased, and they called into question the utility of Markovian master equations that predict only decay. Since Table 1 shows that the LDM method gives significantly less robust results in the diabatic representation,

Table 2. Average Unsigned Percentage Errors in All Six Observables for GCS and CS Switching Schemes and the D Criterion for Strong Interaction Regions^a

			MXH	MCH	YRH	overall
NLDM	a	GCS	21	33	66	40
		CS ^a	24	34	17	25
	d	GCS	17	29	389	145
		CS ^a	19	28	32	26
LDM	a	GCS	21	34	67	41
		CS	21	33	18	24
	d	GCS	22	30	661	238
		CS	24	29	61	38
PDDM	a	GCS	21	33	61	38
		CS	23	32	18	24
	d	GCS	18	29	453	167
		CS	21	28	47	32

^a This is equivalent to original CSDM.

we are hesitant to recommend it for electronically nonadiabatic processes, although it should be noted that if one uses the L criterion in the diabatic representation, the LDM results are good.

Table 2 also shows some results for global coherent switching (GCS). This scheme is interesting because it is the scheme that has always been used in TFS and FSTUVV surface hopping calculations. It works well for the MXH and MCH systems, and GCS switching in both adiabatic and diabatic representations is about as accurate as CS switching for these cases. However, GCS switching is inaccurate for the YRH system.

The full results in Supporting Information confirm that the CS prescription is the best switching algorithm as concluded¹⁶ previously. The self-consistent switching (SCS) algorithm works almost as well as the CS algorithm for the MXH and MCH systems and it shows very good results for the YRH system when simulations are done in the adiabatic representation, but SCS shows poorer results when YRH simulations are carried out in the diabatic representation. The natural switching (NS) algorithm shows the same tendencies as the SCS algorithm, except that NS shows more representation dependence than SCS for the YRH systems. The full tables in Supporting Information also show that all three decay-of-mixing methods (NLDM, LDM, and PDDM) have similar behavior when used with the same switching algorithm. The results are more dependent on the choice of switching algorithm than on the choice of the decay-of-mixing method.

Next, we consider how fast or slow the system decoheres. The region where the trajectory has negligible nonadiabatic and/or diabatic coupling is not interesting. Therefore, we average the decay time only over the portions of the trajectories where $0.02 \leq \rho_{kk} \leq 0.98$. Recall that τ_{kk} is, except for a factor of 2, the reciprocal of a first-order rate constant, and we therefore average the rates, $1/\tau_{12}$, not the decay times. The result is re-expressed in time units by taking a reciprocal, i.e.

$$\bar{\tau} \equiv \frac{1}{\langle 1/\tau_{12} \rangle} \quad (32)$$

Table 3. Mean Decay of Mixings Times (fs) for the CS Switching Algorithm with the NLDM, LDM, and PDDM Decay of Mixing Schemes^a

	MXH (SB)	MXH (WL)	MCH (SB)	MCH (WL)	YRH(0.2)
rep	$j = 0$	$j = 0$	$j = 0$	$j = 0$	$E = 1.02$ eV
Nonlinear Decay of Mixing (NLDM)					
a	7.8(57)	8.5(52)	8.0(37)	26.7(53)	34.8(76)
d(D)	9.5(57)	7.4(52)	9.4(37)	10.9(53)	35.2(84)
d(S)	9.5(67)	7.4(51)	9.4(44)	10.9(54)	35.3(84)
d(L)	9.4(103)	7.4(74)	9.4(79)	10.8(79)	35.4(61)
Linear Decay of Mixing (LDM)					
a	7.7(56)	8.3(53)	7.9(38)	25.9(54)	34.4(77)
d(D)	9.6(66)	7.3(5)	9.2(38)	10.8(53)	34.4(85)
d(S)	9.6(70)	7.4(51)	9.2(44)	10.8(54)	34.4(85)
d(L)	9.4(109)	7.4(74)	9.0(77)	10.7(80)	34.5(63)
Population-Driven Decay of Mixing (PDDM)					
a	7.8(50)	8.6(52)	7.8(37)	26(54)	34.4(76)
d(D)	9.4(57)	7.3(52)	9.1(37)	10.2(53)	35.0(83)
d(S)	9.4(65)	7.3(52)	9.1(44)	10.2(55)	35.0(83)
d(L)	9.2(101)	7.3(75)	9.0(78)	10.3(80)	35.0(61)

^a Numbers in parentheses are the average number of minima of D, S, or L per trajectory.

The results for the CS switching algorithm with NLDM, LDM, and PDDM decay of mixing methods are shown for five of the 17 cases in Table 3. Notice that the average decay-of-mixing time is slightly shorter in the adiabatic representation than in the diabatic representation for MXH (SB) with $j = 0$ and MCH (SB) with $j = 0$, but the average decay-of-mixing time is much longer in the adiabatic representation than in the diabatic representation for MXH (WL) with $j = 0$ and MCH (WL) with $j = 0$. For YRH (0.2) with $j = 0$ the average decay-of-mixing is about the same. NLDM, LDM, and PDDM decay of mixing methods give similar average decay-of-mixing times. For the MXH (SB) and MCH (SB) cases with $j = 0$, the Calaveras County representation is the adiabatic representation, while for the MXH (WL) and MCH (WL) cases with $j = 0$, the Calaveras County representation is the diabatic representation. The examples in Table 3 show that the representation with the shorter average decay-of-mixing time corresponds to the Calaveras County representation for the crossing and conical intersection cases of nonadiabatic transitions. For the noncrossing cases, the average decay-of-mixing times are about the same.

Since the method of comparing semiclassical calculations to quantum ones is improved in this paper (as compared to our previous ones), we also compared other semiclassical results to the quantum ones by precisely the same procedure. Table 4 compares the overall errors for the present methods to trajectory surface hopping and the semiclassical Ehrenfest method. The improvement is significant. Again, it is not necessary to include computation costs since the cost for all methods in the table are similar.

VII. Concluding Remarks

The decay of mixing (DM) formalism¹⁸ was developed by adding decoherence to the semiclassical Ehrenfest method and has been shown to be more accurate than surface hopping methods for non-Born-Oppenheimer collisions. In this article,

Table 4. Comparison of Average Unsigned Percentage Errors of Present Methods to Those for Trajectory Surface Hopping and Ehrenfest Methods

method	rep	MXH	MCH	YRH	overall
ECP ^a	a	97	49	201	116
	d	117	55	495	222
TFS+ ^b	a	64	48	29	47
	d	51	40	361	151
FSTU ∇ ^c	a	52	52	24	43
	d	28	36	125	63
SE ^d	a	65	55		
	d	65	55		
CSDM	a	24	34	17	25
	d(D)	19	28	32	26
CSDM/L	a	21	33	18	24
	d(L)	23	29	30	27
CSDM/PD	a	23	32	18	24
	d(L)	20	29	22	24

^a Exact complete passage trajectory surface hopping method of Parlant and Gislason. ^b Tully's fewest-switches trajectory surface hopping method. Note that we denote this as TFS+ because frustrated hops are ignored in the original method, and in a notation established in earlier articles,^{16,33} this is denoted by a + sign. Originally (refs 82 and 31), we denoted this as ++. ^c Fewest switches with time uncertainty and grad V criterion for frustrated hops (trajectory surface hopping). ^d Semiclassical Ehrenfest. Mean errors cannot be computed for YRH because SE incorrectly predicts no reactive or quenching trajectories for two of the three YRH cases.

we have tested the sensitivity of the DM method to details of how decoherence is introduced into the off-diagonal elements of the density matrix and how the switching probability is computed. The comparison of our previous coherent switches with decay of mixing (CSDM) method to the new methods shows that CSDM is very robust with respect to details of the implementation. In particular, numerical tests based on ensembles of trajectories show that allowing for new forms of decoherence and changes in the switching algorithm do not lead to significant overall improvement, although we can achieve an average improvement of a couple of percentage points.

Although the present article only involves two-state applications, all methods are applicable to general multistate cases. The new methods presented here complement the older methods in that we now have a series of methods with various levels of coherence and decoherence. (The PDDM method is more coherent than the LDM method, and the LDM method has similar coherence to the NLDM method. Among the four switching algorithms, GCS is the most coherent, CS is less, SCS is even less, and NS is the least coherent.) This may help us to better understand the physical nature of decoherence.

Acknowledgment. The authors are grateful to Shikha Nangia for many helpful contributions and to David Micha for helpful suggestions. This work was supported in part by the National Science Foundation under grant no. CHE03-49122.

Supporting Information Available: A list of acronyms and abbreviations, mean unsigned errors not reported in the text, mean decay of mixing times, quantum mechanical

results, and semiclassical trajectory results. This material is available free of charge via the Internet at <http://pubs.acs.org>.

References

- (1) Bunker, D. L. *Methods Comput. Phys.* **1971**, *10*, 287.
- (2) Truhlar, D. G.; Muckerman, J. T. In *Atom-Molecule Collision Theory: A Guide for the Experimentalist*; Bernstein, R. B., Ed.; Plenum: New York, 1979; p 505.
- (3) (a) Allen, M. P.; Tildesley, D. J. *Computer Simulation of Liquids*; Clarendon Press: Oxford, 1987. (b) Brooks, C. L., III; Karplus, M.; Pettit, B. M. *Adv. Chem. Phys.* **1988**, *71*, 1. (c) Benjamin, I. In *Modern Methods for Multidimensional Dynamics Computations in Chemistry*; Thompson, D. L., Ed.; World Scientific: Singapore, 1998; p 101. (d) Stanton, R. V.; Miller, J. L.; Kollman, P. A. In *Modern Methods for Multidimensional Dynamics Computations in Chemistry*; Thompson, D. L., Ed.; World Scientific: Singapore, 1998; p 255. (e) Rice, B. M. In *Modern Methods for Multidimensional Dynamics Computations in Chemistry*; Thompson, D. L., Ed.; World Scientific: Singapore, 1998; p 472.
- (4) For recent review papers, see: (a) Tully, J. C. In *Modern Methods for Multidimensional Dynamics Computations in Chemistry*, Thompson, D. L., Ed.; World Scientific: Singapore, 1998; p 34. (b) Ben-Nun, M.; Martinez, T. J. *Adv. Chem. Phys.* **2002**, *121*, 439. (c) Jasper, A. W.; Kendrick, B. K.; Mead, C. A.; Truhlar, D. G. In *Modern Trends in Chemical Reaction Dynamics, Part I*; Yang, X., Liu, K., Eds.; World Scientific: Singapore, 2004; pp 329–392. (d) Worth, G. A.; Robb, M. A. *Adv. Chem. Phys.* **2002**, *124*, 355. (e) Zhu, C.; Mil'nikov, G. V.; Nakamura, H. In *Modern Trends in Chemical Reaction Dynamics, Part I*; Yang, X., Liu, K., Eds.; World Scientific: Singapore, 2004; pp 393–473. (f) Jasper, A. W.; Zhu, C.; Nangia, S.; Truhlar, D. G. *Faraday Discuss.* **2004**, *127*, 1. (g) Stock, G.; Thoss, M. In *Electronic Structure, Dynamics and Spectroscopy*; Domcke, W., Yarkony, D. R., Köppel, H., Eds.; World Scientific: Singapore, 2004; p 619.
- (5) (a) Sakurai, J. J. *Modern Quantum Mechanics*; Addison-Wesley: Redwood City, CA, 1985. (b) Bohm, A. *Quantum Mechanics: Foundations and Applications*, 3rd ed.; Springer-Verlag: New York, 1993; p 64. (c) Gottfried, K.; Yan, T.-M. *Quantum Mechanics: Fundamentals*, 2nd ed.; Springer: New York, 2003; p 46.
- (6) (a) Fano, U. *Rev. Mod. Phys.* **1957**, *29*, 74. (b) Blum, K. *Density Matrix Theory and Applications*; Plenum: New York, 1981. (c) Schatz, G. C.; Ratner, M. A. *Quantum Mechanics in Chemistry*; Prentice Hall: Englewood Cliffs, 1993; p 277. (d) May, V.; Kühn, O. *Charge and Energy Transfer Dynamics in Molecular Systems*; Wiley-VCH: Berlin, 2000; p 73.
- (7) (a) Johnson, C. S., Jr.; Tully, J. C. *J. Chem. Phys.* **1964**, *40*, 1764. (b) Coalson, R. D.; Karplus, M. *J. Chem. Phys.* **1983**, *79*, 6150. (c) Bittner, E. R.; Light, J. C. *J. Chem. Phys.* **1994**, *101*, 2446. (d) Berman, M.; Kosloff, R.; Tal-Ezer, H. *J. Phys. A* **1992**, *25*, 1283. (e) Pesce, L.; Saalfrank, P. *J. Chem. Phys.* **1998**, *108*, 3045. (f) Guo, H.; Chen, R. *J. Chem. Phys.* **1999**, *110*, 6626. (g) Costella, F. J. *Stat. Phys.* **2001**, *104*, 387. (h) Kristensen, J. H.; Hoatson, G. L.; Vold, R. L. *J. Comput. Phys.* **2001**, *170*, 415. (i) Horenko, I.; Weiser, M.; Schmidt, B.; Schütte, C. *J. Chem. Phys.* **2004**, *120*, 8913. (j) Shi, Q.; Geva, E. *J. Chem. Phys.* **2004**, *121*, 3393.
- (8) Mukamel, S. *Principles of Nonlinear Optical Spectroscopy*; Oxford University Press: New York, 1995.
- (9) Beksic, D.; Micha, D. A. *J. Chem. Phys.* **1995**, *103*, 3795.

- (10) Bittner, E. R.; Rossky, P. J. *J. Chem. Phys.* **1995**, *103*, 8130.
- (11) Ashkenaz, G.; Kosloff, R.; Ratner, M. A. *J. Am. Chem. Soc.* **1999**, *121*, 3386.
- (12) Prezhdo, O. V. *Phys. Rev. Lett.* **2000**, *85*, 4413.
- (13) Santer, M.; Manthe, U.; Stock, G. *J. Chem. Phys.* **2001**, *114*, 2001.
- (14) Prezhdo, O. V.; Rossky, P. J. *J. Chem. Phys.* **1997**, *107*, 5863.
- (15) Zhu, C.; Jasper, A. W.; Truhlar, D. G. *J. Chem. Phys.* **2004**, *120*, 5543.
- (16) Zhu, C.; Nangia, S.; Jasper, A. W.; Truhlar, D. G. *J. Chem. Phys.* **2004**, *121*, 7658.
- (17) Wong, K. F.; Rossky, P. J. *J. Chem. Phys.* **2002**, *116*, 8418, 8429.
- (18) Hack, M. D.; Truhlar, D. G. *J. Chem. Phys.* **2001**, *114*, 9305.
- (19) (a) Burant, J. C.; Tully, J. C. *J. Chem. Phys.* **2000**, *112*, 6097. (b) Wan, C. C.; Schofield, J. *J. Chem. Phys.* **2002**, *116*, 494. (c) Ben-Num, M.; Martinez, T. J. *Adv. Chem. Phys.* **2002**, *121*, 439. (d) Donoso, A.; Zheng, Y.; Martens, C. C. *J. Chem. Phys.* **2003**, *119*, 5010. (e) Roman, E.; Martens, C. C. *J. Chem. Phys.* **2004**, *121*, 11572.
- (20) Tully, J. C.; Preston, R. K. *J. Chem. Phys.* **1971**, *55*, 562.
- (21) Blais, N. C.; Truhlar, D. G. *J. Chem. Phys.* **1983**, *79*, 1334.
- (22) Parlant, G.; Gislason, E. A. *J. Chem. Phys.* **1989**, *91*, 4416.
- (23) Parlant, G.; Alexander, M. H. *J. Chem. Phys.* **1990**, *92*, 2287.
- (24) Tully, J. C. *J. Chem. Phys.* **1990**, *93*, 1061.
- (25) Coker, D. F.; Xiao, L. *J. Chem. Phys.* **1995**, *102*, 496.
- (26) Topaler, M. S.; Hack, M. D.; Allison, T. C.; Liu, Y.-P.; Mielke, S. L.; Schwenke, D. W.; Truhlar, D. G. *J. Chem. Phys.* **1997**, *106*, 8699.
- (27) Sizun, M.; Song, J.-B.; Gislason, E. A. *J. Chem. Phys.* **1998**, *109*, 4815.
- (28) Hack, M. D.; Jasper, A. W.; Volobuev, Y. L.; Schwenke, D. W.; Truhlar, D. G. *J. Phys. Chem. A* **1999**, *103*, 6309.
- (29) Babikov, D.; Gislason, E. A.; Sizun, M.; Aguillon, F.; Sidis, V. *J. Chem. Phys.* **2000**, *112*, 7032.
- (30) Hack, M. D.; Jasper, A. W.; Volobuev, Y. L.; Schwenke, D. W.; Truhlar, D. G. *J. Phys. Chem. A* **2000**, *104*, 217.
- (31) Jasper, A. W.; Stechmann, S. N.; Truhlar, D. G. *J. Chem. Phys.* **2002**, *116*, 5424; **2002**, *117*, 10247(E).
- (32) Zhu, C.; Kamisaka, H.; Nakamura, H. *J. Chem. Phys.* **2002**, *116*, 3234.
- (33) Jasper, A. W.; Truhlar, D. G. *Chem. Phys. Lett.* **2003**, *369*, 60.
- (34) Meyer, H.-D.; Miller, W. H. *J. Chem. Phys.* **1979**, *70*, 3214.
- (35) Kuntz, P. J.; Kendrick, J.; Whitton, W. N. *Chem. Phys.* **1979**, *38*, 147.
- (36) Meyer, H.-D.; Miller, W. H. *J. Chem. Phys.* **1980**, *72*, 2272.
- (37) Micha, D. A. *J. Chem. Phys.* **1983**, *78*, 7138.
- (38) Amarouche, M.; Gadea, F. X.; Durup, J. *Chem. Phys.* **1989**, *130*, 145.
- (39) Garcia-Vela, A.; Gerber, R. B.; Imre, D. G. *J. Chem. Phys.* **1992**, *97*, 7242.
- (40) Billing, G. D. *Int. Rev. Phys. Chem.* **1994**, *13*, 309.
- (41) Kohen, D.; Stillinger, F. H.; Tully, J. C. *J. Chem. Phys.* **1998**, *109*, 4713.
- (42) Thachuk, M.; Ivanov, M. Y.; Wardlaw, D. M. *J. Chem. Phys.* **1998**, *109*, 5747.
- (43) Micha, D. A. *Adv. Quantum Chem.* **1999**, *35*, 317.
- (44) Yalobuev, Y. L.; Hack, M. D.; Truhlar, D. G. *J. Phys. Chem. A* **1999**, *103*, 6225.
- (45) Mavri, J. *Mol. Simul.* **2000**, *23*, 389.
- (46) Hack, M. D.; Jasper, A. W.; Volobuev, Y. L.; Schwenke, D. W.; Truhlar, D. G. *J. Phys. Chem. A* **2000**, *104*, 217.
- (47) Volobuev, Y. L.; Hack, M. D.; Topaler, M. S.; Truhlar, D. G. *J. Chem. Phys.* **2000**, *112*, 9716.
- (48) Hack, M. D.; Truhlar, D. G. *J. Phys. Chem. A* **2000**, *104*, 7917.
- (49) Zurek, W. H. *Phys. Rev. D* **1981**, *24*, 1516.
- (50) Zurek, W. H. *Rev. Mod. Phys.* **2003**, *75*, 715.
- (51) Zurek, W. H. *Phys. Rev. D* **1982**, *26*, 1862.
- (52) Zeh, H. D. In *New Developments on Fundamental Problems in Quantum Physics*; Ferrero, M., van der Merwe, A., Eds.; Kluwer: Dordrecht, 1997.
- (53) Zurek, W. H. *Philos. Trans. R. Soc. London, Ser. A* **1998**, *356*, 1793.
- (54) Stock, G. *Phys. Rev. E* **1995**, *51*, 2004.
- (55) (a) Nakajima, S. *Prog. Theor. Phys.* **1958**, *20*, 948. (b) Zwanzig, R. *Physica* **1964**, *30*, 1109.
- (56) (a) Feynman, R. P.; Vernon, F. L., Jr. *Ann. Phys. (N.Y.)* **1963**, *24*, 118. (b) Caldeira, A. O.; Leggett, A. J. *Physica A* **1983**, *121*, 587.
- (57) Zeh, H. D. *Lect. Notes Phys.* **2000**, *538*, 19.
- (58) (a) Gisin, N.; Percival, I. C. *J. Phys. A* **1992**, *25*, 5677. (b) Diosi, L.; Gisin, N.; Strunz, W. T. *Phys. Rev. A* **1998**, *58*, 1699.
- (59) Anglin, J. R.; Paz, J. P.; Zurek, W. H. *Phys. Rev. A* **1997**, *55*, 4041.
- (60) (a) Bloch, F. *Phys. Rev.* **1946**, *70*, 460. (b) Redfield, A. G. *Adv. Magn. Reson.* **1965**, *1*, 1. (c) Lindblad, G. *Commun. Math. Phys.* **1976**, *48*, 119. (d) Gorini, V.; Kossalowski, A.; Sudarshan, E. C. G. *J. Math. Phys.* **1976**, *17*, 821. (e) Haake, F.; Risken, H.; Savage, C.; Walls, D. *Phys. Rev. A* **1986**, *34*, 3969. (f) Laird, B. B.; Budimir, J.; Skinner, J. L. *J. Chem. Phys.* **1991**, *94*, 4391. (g) Suarez, A.; Silbey, R.; Oppenheim, I. *J. Chem. Phys.* **1992**, *97*, 5101. (h) Diosi, L.; Kiefer, C. *Phys. Rev. Lett.* **2000**, *85*, 3552. (i) Zhao, Y.; Chen, G. H. *J. Chem. Phys.* **2001**, *114*, 10623.
- (61) (a) Hu, B. L.; Paz, J. P.; Zhang, Y. *Phys. Rev. D* **1992**, *45*, 2843. (b) Hu, B. L.; Paz, J. P.; Zhang, Y. *Phys. Rev. D* **1993**, *47*, 1576.
- (62) (a) Lindblad, G. *J. Phys. A* **1996**, *29*, 4197. (b) Makri, N. J. *J. Phys. Chem. A* **1998**, *102*, 4414. (d) Meier, C.; Tannor, D. J. *J. Chem. Phys.* **1999**, *111*, 3365. (d) Burghardt, I. *J. Chem. Phys.* **2001**, *114*, 89. (e) Wilkie, J. J. *J. Chem. Phys.* **2001**, *114*, 7736. (f) Shi, Q.; Geva, E. *J. Chem. Phys.* **2003**, *119*, 12063. (g) Rau, A. R. P.; Zhao, W. *Phys. Rev. A* **2003**, *68*, 52102. (h) Kleinekathoefer, J. *Chem. Phys.* **2004**, *121*, 2505. (i) Shi, G.; Geva, E. *J. Chem. Phys.* **2004**, *121*, 3393. (j) Lee, J.; Kim, I.; Ahn, D.; McAneney, H.; Kim, M. S. *Phys. Rev. A* **2004**, *70*, 24301.
- (63) Mead, C. A.; Truhlar, D. G. *J. Chem. Phys.* **1982**, *77*, 6090.

- (64) Nakamura, H.; Truhlar, D. G. *J. Chem. Phys.* **2001**, *115*, 10353.
- (65) Kuppermann, A.; Abrol, R. *Adv. Chem. Phys.* **2002**, *124*, 283.
- (66) Köppel, H. In *Conical Intersections: Electronic Structure, Dynamics and Spectroscopy*; Domcke, W., Yarkony, D. R., Köppel, H., Eds.; World Scientific: Singapore, 2004; p 175.
- (67) Kleckner, M.; Ron, A. *Phys. Rev. A* **2001**, *63*, 22110.
- (68) Kohen, D.; Tannor, D. J. *J. Chem. Phys.* **1997**, *107*, 5141.
- (69) Elran, Y.; Brumer, P. *J. Chem. Phys.* **2004**, *121*, 2673.
- (70) Sinha, S. *Phys. Lett. A* **1997**, *228*, 1.
- (71) Allison, T. C.; Truhlar, D. G. In *Modern Methods for Multidimensional Dynamics Computations in Chemistry*; Thompson, D. L., Ed.; World Scientific: Singapore, 1998; p 618.
- (72) Landau, L. D. *Phys. Z. Sowjet.* **1932**, *2*, 46.
- (73) Zener, C. *Proc. R. Soc. London Ser. A* **1932**, *137*, 696.
- (74) Stückelberg, E. C. G. *Helv. Phys. Acta* **1932**, *5*, 369.
- (75) Teller, E. *J. Phys. Chem.* **1937**, *41*, 109.
- (76) Longuet-Higgins, H. C. *Adv. Spectrosc.* **1961**, *2*, 429.
- (77) Herzberg, G. *Electronic Spectra and Electronic Structure of Polyatomic Molecules*; van Nostrand Reinhard: New York 1966; p 442.
- (78) Jasper, A. W.; Truhlar, D. G. *J. Chem. Phys.* **2005**, *22*, 044101.
- (79) Rosen, N.; Zener, C. *Phys. Rev.* **1932**, *18*, 502.
- (80) Demkov, Y. N. *Zh. Eksp. Teor. Fiz.* **1963**, *45*, 195 [English transl.: *Sov. Phys. JETP* **1964**, *18*, 138].
- (81) Osherov, V. L.; Voronin, A. L. *Phys. Rev. A* **1994**, *49*, 265.
- (82) Jasper, A. W.; Hack, M. D.; Truhlar, D. G. *J. Chem. Phys.* **2001**, *115*, 1804.
- (83) Press, W. H.; Teukolsky, S. A.; Vetterling, W. T.; Flannery, B. P. *Numerical Recipes in Fortran*, 2nd ed; Cambridge University Press: Cambridge, U.K., 1994; p 716.
- (84) Zhu, C.; Nangia, S.; Jasper, A. W.; Volobuev, Y.; Topaler, M. S.; Allison, T. C.; Hack, M. D.; Liu, Y.-P.; Anderson, A. G.; Stechmann, S. N.; Miller, T. F., III; Blais, N. C.; Truhlar, D. G. NAT-version 8.1, University of Minnesota, 2004.
- (85) Topaler, M. S.; Allison, T. C.; Schwenke, D. W.; Truhlar, D. G. *J. Chem. Phys.* **1998**, *109*, 3321; **1999**, *110*, 687(E).

CT050021P